

# Highly photocatalyst efficient in LEDs/solar active and reusable: Sm–ZnO–Ag nanoparticles for methylene blue degradation

Yesuvadimai Jerlin Jose<sup>1,3</sup> · Munisamy Manjunathan<sup>1,2</sup>  · Savariraj Joseph Selvaraj<sup>3</sup>

Received: 7 May 2017 / Accepted: 17 July 2017 / Published online: 29 July 2017  
© The Author(s) 2017. This article is an open access publication

**Abstract** The precipitation–decomposition method was used to prepare the photocatalyst (Sm–ZnO–Ag). Synthesized catalyst was characterized by X-ray diffraction, field emission scanning electron microscope images, and optical spectroscopy. The activity of photocatalyst of Sm–ZnO–Ag was checked for the photodegradation of thiazin-type methylene blue (MB) dye in aqueous solution using light emitting diodes/solar illumination. Sm–ZnO–Ag is found to be excellent competent than Ag–ZnO, Sm–ZnO and ZnO nanoparticles. The absorbance of ZnO was shifted into the visible region by the dopants (Ag and Sm). The

influences of operational parameters such as initial pH, dose of photocatalyst and dye concentration on photomineralization of MB have been analyzed. Sunlight (16 min) gives excellent results in photocatalytic degradation compared to LED (80 min). The microbial zones of Sm–ZnO–Ag (Nps) showed free radical generation. The Sm–ZnO–Ag catalyst is stable and it's reusable. A degradation mechanism is proposed for the photodegradation of MB under LED/solar light.

---

**Electronic supplementary material** The online version of this article (doi:[10.1007/s40097-017-0236-3](https://doi.org/10.1007/s40097-017-0236-3)) contains supplementary material, which is available to authorized users.

---

✉ Munisamy Manjunathan  
manjunath876@gmail.com

Yesuvadimai Jerlin Jose  
y.josechem@gmail.com

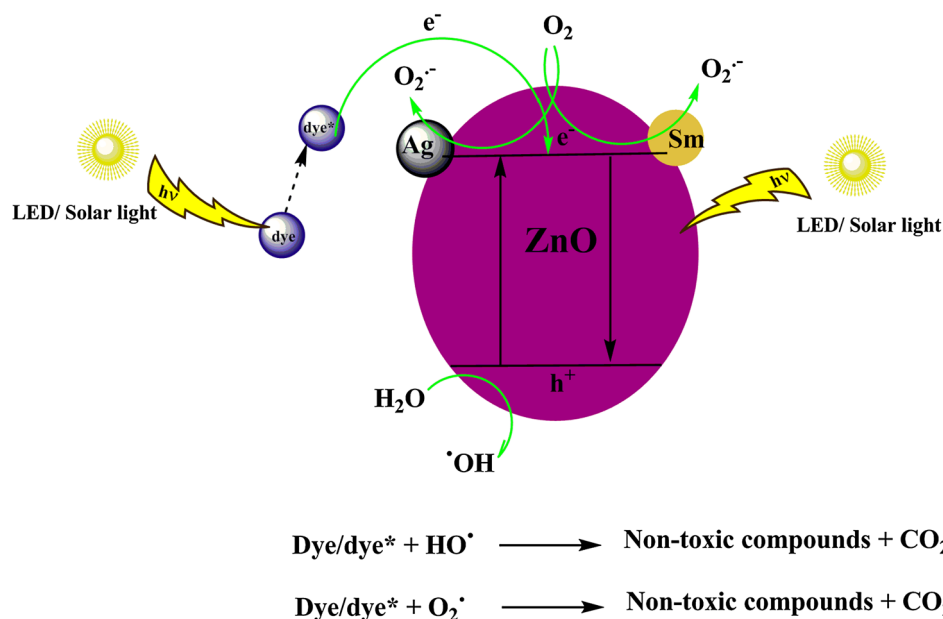
Savariraj Joseph Selvaraj  
sjc\_selvaraj@yahoo.com

<sup>1</sup> Department of Chemistry, BWDA Arts and Science College, Tindivanam 604304, India

<sup>2</sup> Department of Chemistry, Pondicherry University, Pondicherry 605014, India

<sup>3</sup> Department of Chemistry, St. Josephs College, Tiruchirappalli 620002, India

## Graphical Abstract



**Keywords** Photodegradation · Nanoparticles · Sunlight · LEDs · MB

## Introduction

Pollution occurs from various factors, one of them being from water which plays a vital role in our day to day life. 90% of the world is surrounded by water and is the most important source for survival of all living organisms. It is also required for industrial, agricultural and domestic sectors. This polluted water consists of a large number of toxic chemicals such as solvent, dyes, pesticides polychlorinated biphenyls (PCB), chlorophenol, heavy metals, arsenic and asbestos [1, 2]. A dye containing waste water is released from industries, especially from fabrics, leather industries, etc. This contains many non-reactive raw materials such as organic amines, inorganic and organometallic substances, and dissipates solvents which are found in different concentrations, and this water then becomes unusable. Once the dyes are decomposed, that water can be utilized for other purposes. If any living being use this polluted water, it would lead to severe harm. The adverse effects are broad-ranging immune suppression, behavioral problems, tissue necrosis infection of skin and eyes, breath problems, CNS dissolves and all organic reactions [3] Dyes not only damage the human life, but also the aquatic life [4, 5]. It does not decompose in water, because of their complicated chemical composition [6]. They are resistant to biodegradation [7, 8]. There are numerous methods which are used to remove the dyes from water, among this oxidation process is an important one. It degrades the dyes with the

help of  $\text{HO}^\bullet$  radical [9], but this method requires eminent energy light irradiation source (UV light) and on oxidant. The process which is currently available till now is UV/ $\text{H}_2\text{O}_2$ , UV/Ozone, UV/Fenton reagent, and UV/semiconductor [10].

Currently, photocatalytic degradation is an advanced method in the existence of natural solar light or mercury vapor lamp [11, 12], as they are an efficient light source for photodegradation. LED can emit light at different wavelengths based on semiconductor material. It contains monochromatic light and it can be used for higher brightness and single color radiation. It is non-toxic and environmentally friendly. LEDs are far more efficient than incandescent lamps at converting electricity into visible light while being robust and small. It is a very good alternative for UV traditional. The highest amount of light generated by most LEDs is around its peak wavelength [13, 14]. ZnO Nps play a vital role because the degradation is much more powerful on toxic chemicals. ZnO Nps absorb the UV light approximately of wavelength 385 nm. The wavelength of the visible light is between 400 and 700 nm. Moreover, ZnO Nps shows quick reunion of photo-induced electrons and holes which reduces the catalytic activity. So catalyst needs to be improved by the addition of dopants. From the conduction band, these dopants on a catalytic surface can efficiently capture the electrons. Therefore, ZnO Nps should be a promising alternative for  $\text{TiO}_2$  in photocatalysis [15–20].

Recently, two different atoms were doped into catalytic semiconductor, which gives an excellent photocatalytic activity better than a single dopant into the semiconductor oxides such as  $\text{Ag}^+$  and  $\text{La}^{3+}$  [21]. Among the other

lanthanides, [22] Sm-doped ZnO has excellent activity due to  $\text{Sm}^{3+}/\text{Sm}^{2+}$  redox couple. The doping of transition and rare earth ions on the ZnO produces impure energy levels in band gap and spread out its visible light response; furthermore, it produces traps for photogenerated charge carriers, therefore, accelerating the interfacial charge transfer and inhibiting the recombination of electron–hole pairs [23, 24]. Similar activity is observed in Ce [25], Zr [26] Co doped with Ag–ZnO nanoparticles showed the excellent photocatalytic activity for the degradation of dyestuffs. This study shows precipitation–decomposition method for the synthesis of Sm–ZnO–Ag nano-photocatalysts. These materials demonstrate the catalytic activity and its stability for photodegradation of methylene blue with LED/sunlight illumination, among this a possible mechanisms of photodegradation has been described.

## Experimental

### Materials and methods

All the reagents taken in this work are of AR grade and used as it is. The commercial thiazin dye, methylene blue (MB), obtained (molecular formula =  $\text{C}_{16}\text{H}_{18}\text{ClN}_3\text{S}$ ; molecular mass in amu 319.86 and  $\lambda_{\text{max}}$  644 nm),  $\text{C}_2\text{H}_2\text{O}_4 \cdot 2\text{H}_2\text{O}$  (99%) and  $\text{Zn}(\text{NO}_3)_2 \cdot 6\text{H}_2\text{O}$  (AR),  $\text{AgNO}_3$  and  $\text{SmCl}_3 \cdot 6\text{H}_2\text{O}$  have been obtained from Sigma-Aldrich and Merck. Distilled water is taken to prepare experimental (alkaline  $\text{KMnO}_4$ ) solutions. Proper pH is maintained by adding acid or base before irradiation of the solution.

### Preparation of Sm–ZnO–Ag Nps

Modified method [25] of photocatalyst was prepared by a precipitation–decomposition method (Scheme 1); 100 mL of 0.5 M  $\text{Zn}(\text{NO}_3)_2 \cdot 6\text{H}_2\text{O}$  and 100 mL of 0.7 M ( $\text{H}_2\text{C}_2\text{O}_4 \cdot 2\text{H}_2\text{O}$ ) were prepared with distilled water and heated to 60 °C separately. 5 ml of  $7.5 \times 10^{-4}$  M of  $\text{AgNO}_3$  solution and 5 ml of samarium chloride hexahydrate ( $\text{SmCl}_3 \cdot 6\text{H}_2\text{O}$ ) solution both were added drop by drop into zinc nitrate solution. After that, oxalic acid was poured slowly into cationic ( $\text{Zn}^{2+} + \text{Ag}^+ + \text{Sm}^{3+}$ ) mixture with constant agitation (pH = 5–6), and then warmed for 1 h at 70 °C. The precipitated solution was cooled down to 30 °C. A homogeneous precipitate of Sm and Ag–Zn $\text{C}_2\text{O}_4$  was obtained. The distilled water was used to wash the formed precipitate Sm and Ag–zinc oxalate precipitate several times and air-dried for minimum 12 h. Then the precipitate was dried at 100 °C for 5 h. The muffle furnace was used in the calcination process to reach decomposition temperature 450 °C at the rate of 10 °C min. The muffle furnace was cooled to room temperature after 10 h. Then, a

complete analysis of Sm–ZnO–Ag Nps was done. The prepared catalyst was 8 wt% of Sm. The same procedure was followed to prepare catalyst with 2 and 4 wt% of Sm. The bare ZnO and silver-doped ZnO were obtained by the above procedure with necessary chemicals.

### Analytical methods

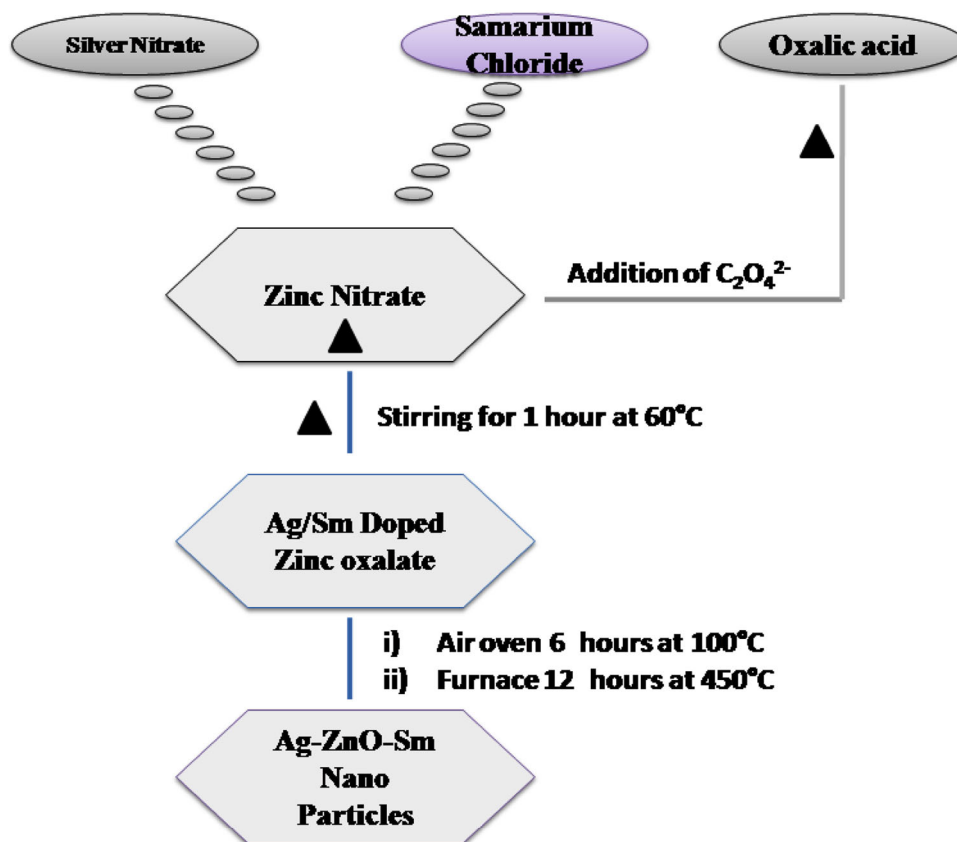
Powder X-ray diffraction pattern was obtained using an X'Pert PRO diffractometer equipped with Cu–K $\alpha$  radiation (wavelength = 1.5406 Å) at 2.2 kW (max); peak positions were compared with standard files to identify the crystalline phases. The morphology of the samples was examined using a JEOL JSM-6701F field emission scanning electron microscope (FE-SEM). Before FE-SEM measurements, the samples were mounted on a gold platform placed in the scanning electron microscope for subsequent analysis at various magnifications, equipped with OXFORD, energy dispersive X-ray microanalysis (EDS). Room temperature PL was recorded with a Horiba JobinYvon, SPEX-SF13-11 spectrofluorometer using 450 nm excitation from xenon lamp. UV–Visible absorbance and diffuse reflectance spectra were recorded in Shimadzu, (UV 2450) double-beam spectrophotometer, equipped with integrating sphere attachment (ISR- 2200) using  $\text{BaSO}_4$  as the reference. Emission spectra were recorded on Spex FluoroLog-3 spectrofluorometer (JobinYvon Inc.) using 450 W xenon lamp. Time-resolved fluorescence decay measurements were carried out using nano-LED ( $\lambda_{\text{exc}}$  = 295 nm).

### Photodegradation experiments and antimicrobial studies

A photochemical reactor model of (50 × 25) (height × diameter) 60 mL capacity was used for the reaction (model in S6) in this study. The catalyst was magnetically stirred without light for 30 min to reach adsorption–desorption balance between the MB and Sm–ZnO–Ag Nps [50 mL of MB ( $10^{-5}$  M)]. The calculated amount of photocatalyst was stirred for 30 min without light prior to illumination to obtain maximum adsorption of dye onto the catalytic surface. No volatility of the solvent was seen during illumination; a sample without light adsorption was collected. In photochemical reactor, reaction mixture of 50 mL was taken and irradiated with LEDs (UVLEDs) trip peak having 6 W output power and maximum relative intensity of wavelength of 375 nm for each LED, totally 5 sets of photocatalytic reactors, each reactor having 20 LEDs [27, 28] and solar light. At regular time gaps, 3 mL of the degraded sample was taken out and centrifuged to remove the catalyst for further analysis. The same condition was used for solar light (LT Lutron LX-10/A Digital Lux meter and the intensity was  $1250 \times 100 \pm 100$  lx—model in S7) degradation of MB,



**Scheme 1** Schematic representation for the preparation of Sm–ZnO–Ag Nps



the solar light intensity was nearly constant during the experiments done at day time 11 A.M–3 P.M (Tamilnadu, India) [27].

### Antibacterial and antifungal assessment

#### Culture and inoculums

Standard bacterial and fungal cultures, *Escherichia coli*, *Enterococcus faecium*, *Pseudomonas aeruginosa*, *Aspergillus niger* and *Fusarium oxysporum* were procured from Nehru Memorial College, Tamil Nadu, India. The bacterial and fungal cultures were subcultured to check their purity and a single colony was inoculated in 50 ml of nutrient and potato dextrose broth, incubated overnight at 30 °C for further studies [29].

#### Agar diffusion method

The gel diffusion method was used for anti-fungal and bacterial studies. Nutrient broth and potato dextrose broth were affixed with actively growing 100 ml of culture and then allowed it to solidify. Afterwards that, making a well with the help of cork borer. 100 ml of aliquots of 5 mg/ml dispersed doped and undoped ZnO was inoculated into the well and allowed it to incubate for 48 h incubation period

at 300 °C. A zone of clearance around the well was observed for further studies. The diameter against the microbes was determined for all microbes in a similar manner. Average values ensure the reliability of the result.

### Results and discussion

#### XRD analysis

Figure 1 shows that the X-ray diffraction patterns of synthesized photocatalyst are showed in a hexagonal wurtzite structure. It is indicated beside the synthesized product from ZnO peaks. For the bare ZnO, we obtained wurtzite ZnO structure of plane (100) having peak 36.18, plane (002) of peak 34.36, plane (101) of peak 36.18, and plane (110) of peak 56.56. For Ag–ZnO Nps, the Ag concentration was really depressed. The XRD will not detect the Ag (3 wt%) peak because of its lower concentration and the presence of Ag detected by EDAX. No diffraction peaks of Sm was obtained for different concentrations of Sm–ZnO–Ag Nps and no other contamination phases were detected, saying that in ZnO lattices Zn<sup>2+</sup> sites are evenly substitute by Ag<sup>+</sup>/Sm<sup>3+</sup> ions. The peaks obtained from XRD are broader in width and their volumes are weak, this shows that Sm content is increased, and also Sm dopant retards

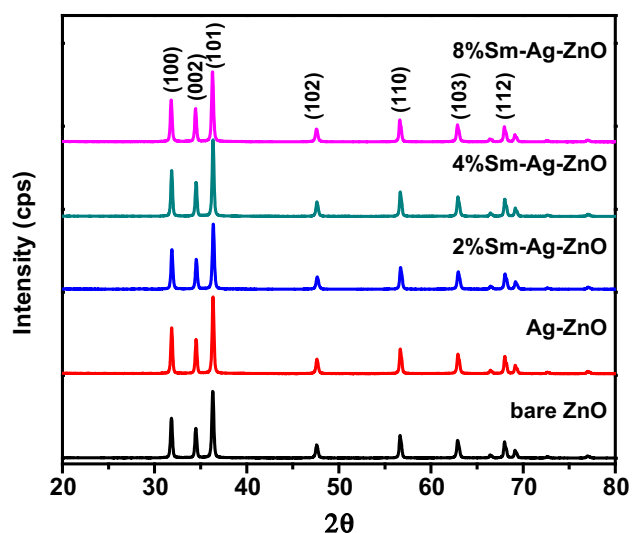


**Fig. 1** XRD patterns of bare ZnO and Sm–ZnO–Ag Nps

the growth of crystal size [30]. The middling sizes of crystals ( $D$ ) of all catalyst are calculated by plane (101) peak value using Scherrer equation  $D = 0.89\lambda/(\beta\cos\theta)$ , here  $\lambda$  is the wavelength of the incident X-ray radiation,  $\beta$  is the full width at half maximum and  $\theta$  is the Bragg angle

[31]. The pure ZnO Nps crystalline size is more than the Ag-doped ZnO and Sm–ZnO–Ag [32].

### FE-SEM analysis

The important and foremost components of characterization are studying the surface morphologies of the synthesized catalyst products. The surface morphology of 8% of Sm–ZnO–Ag studied by FE-SEM images is taken at lower and higher magnifications with various places as showed hexagonal structure is clearly shown at higher magnification (500 nm) of ZnO Nps (Fig. 2). The hexagonal structure is clearly shown at higher magnification (500 nm) of ZnO Nps. The arrow mark indicates the presence of Sm at lower magnification at three different locations (1, 3 and 5  $\mu\text{m}$ ). Sm particles are highly spread over the surface of photocatalyst, similar morphology also observed in 2% and 4% Sm–ZnO–Ag catalyst. EDAX helped to show the elements present in the synthesized catalysts Sm, Ag, Zn and O (Fig. 3).

### The diffuse reflectance spectra

The DRS of bare, Ag–ZnO and Sm–ZnO–Ag are shown in Fig. 4, respectively. The absorbance of ZnO while doping

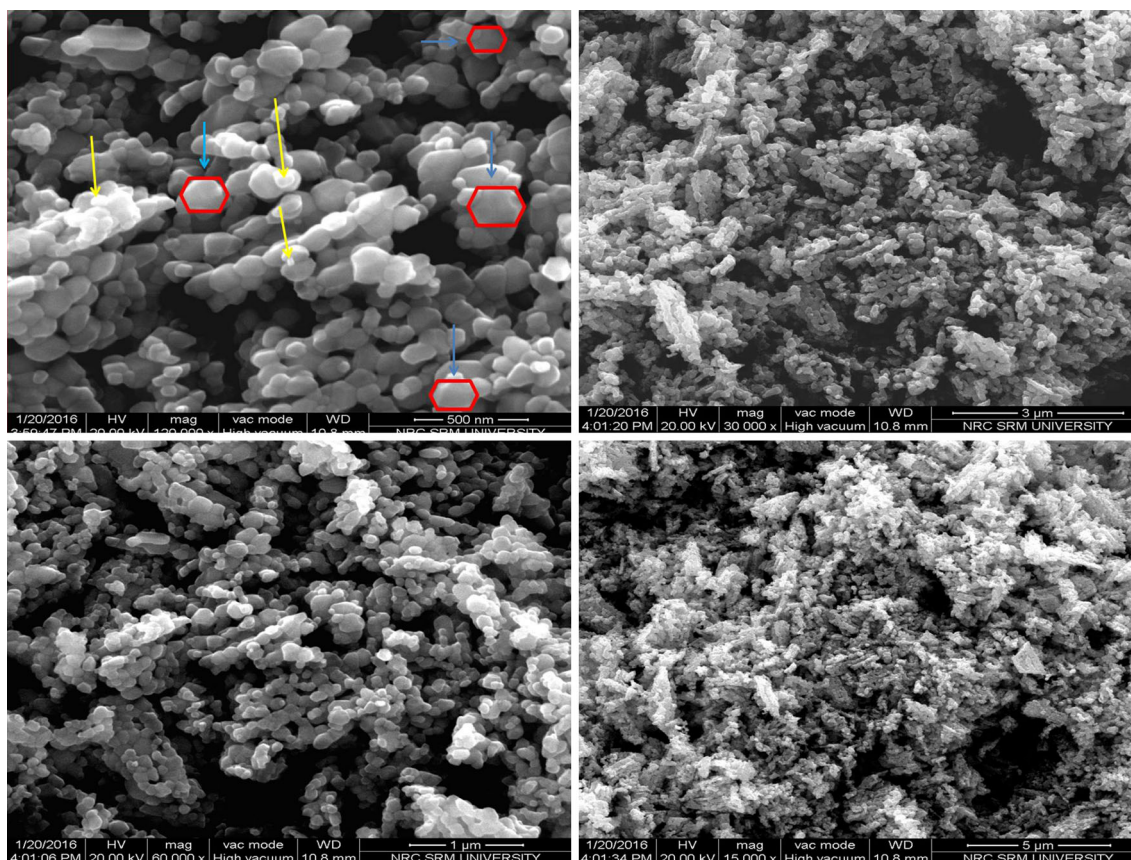


**Fig. 2** FE-SEM images at 8% Sm–ZnO–Ag Nps at different magnifications (500 nm, 1, 3, 5  $\mu\text{m}$ )

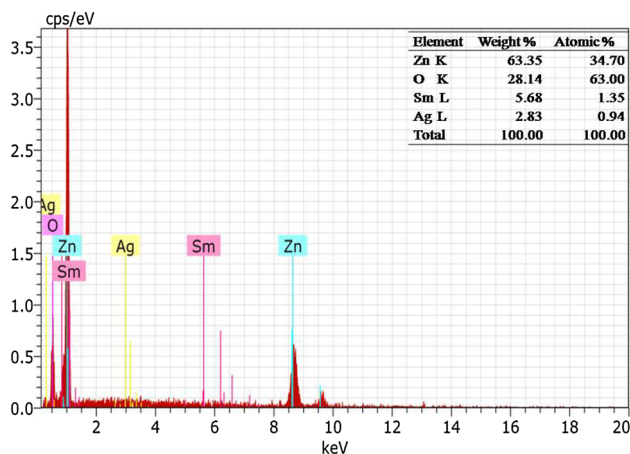


**Fig. 3** EDAX images at 8% Sm–ZnO–Ag Nps

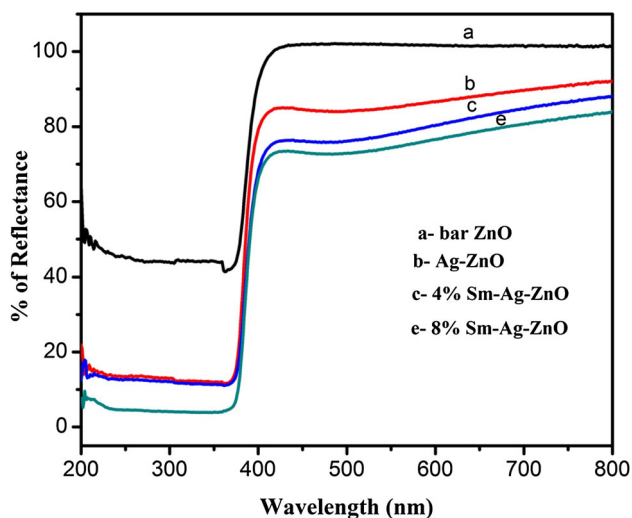


**Fig. 4** Diffuse reflectance spectra of **a** bare ZnO, **b** Ag–ZnO, **c** 4% Sm–ZnO–Ag, and **d** 8% Sm–ZnO–Ag Nps

Sm shifts to the visible region because of the compositment of the dopants Sm and Ag. The absorbance of ZnO shifts to visible region by dopant Sm. The codopants (Ag and Sm) improve the visible light absorbance of ZnO. We could note that Sm–ZnO–Ag is greater than 400 nm (visible region) and that is proved to be greater than pure ZnO. We could observe a slight red shift when compared to pure ZnO Nps; the similar results are absorbed in absorbance spectroscopy (Fig S4). The obtained red shift clearly shows that the sharper band gap is formed, and from Sm ion 4f level to ZnO valence or conduction band there is a charge transfer spectra. The band gap energies are computed by the plot of the customized Kubelka–Munk function (Eq. 1)  $[F(R)E]^{1/2}$  vs the energy of the absorbed light  $E$  and shown in Fig. 5.

$$F(R)E^{1/2} = \left[ (1 - R)^2 hv / 2R \right]^{1/2} \quad (1)$$

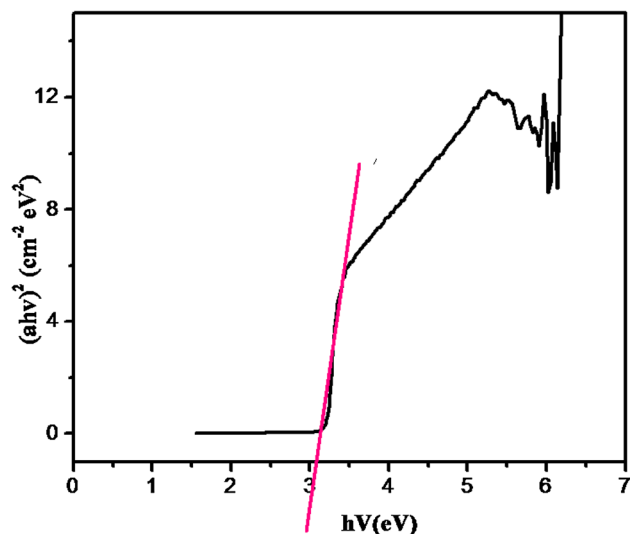


**Fig. 5** Plot for (BG) Kubelka–Munk function vs energy of the light absorbed of the catalyst

The measured band gap is lower than the bare ZnO Nps. The band gap of Sm–ZnO–Ag Nps is 3.02 eV, whereas for bare ZnO Nps is 3.2 eV.

### Photoluminescence spectra

Photogenerated electron and the constitution of a hole in a semiconductor can be studied by PL spectrum. The emission is obtained from the regathering of free charge carriers. If the intensity of PL decreases the electron–hole regathering rate also decreases and in turn increases the photocatalytic activity. Figure 6 shows the PL spectra of the synthesized products. Bare ZnO Nps has higher PL intensity and it decreases from Ag–ZnO Nps to 8% Sm–ZnO–Ag Nps. Bare ZnO Nps gives two emissions at 407

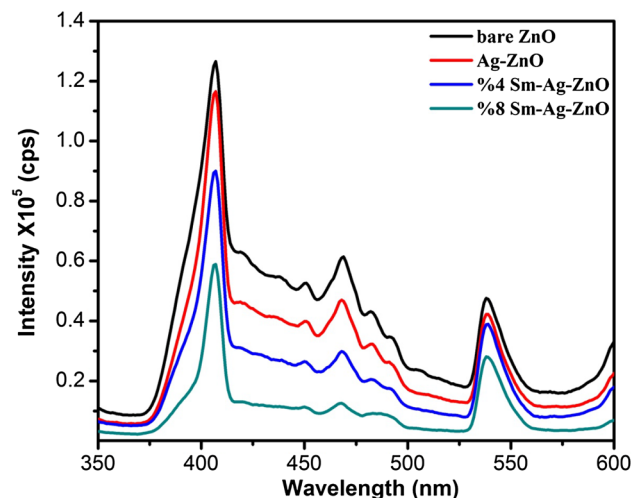


**Fig. 6** Photoluminescence spectra of bare ZnO, Ag–ZnO, 4% Sm–ZnO–Ag, and 8% Sm–ZnO–Ag Nps



**Table 1** Optical properties and average crystalline size of ZnO bare and Sm–ZnO–Ag Nps

| S. no. | Sample id    | $\lambda_{\max}$ (nm) | $E_{\max}$ (nm)/intensity (cps) | Life time (ns) |          |          |                     | Average crystalline size (nm) |
|--------|--------------|-----------------------|---------------------------------|----------------|----------|----------|---------------------|-------------------------------|
|        |              |                       |                                 | $\tau_1$       | $\tau_2$ | $\tau_3$ | $\tau_{\text{ave}}$ |                               |
| 1      | ZnO bare     | 358                   | 407/1,26,572                    | 2.19           | 9.44     | 8.32     | 3.99                | 45.62                         |
| 2      | Ag–ZnO       | 362                   | 407/1,16,546                    | –              |          |          |                     | 22.32                         |
| 3      | 2% Sm–ZnO–Ag | 363                   | 407/92,058                      | 2.44           | 3.18     | 3.45     | 11.8                | 14.93                         |
| 4      | 4% Sm–ZnO–Ag | 363                   | 407/90,032                      | 2.37           | 3.14     | 2.4      | 11.3                | 14.43                         |
| 5      | 8% Sm–ZnO–Ag | 363                   | 407/58,892                      | 2.23           | 3.12     | 2.36     | 11.2                | 15.02                         |

and 537 nm. The doping of Ag and Sm does not change the emission peak, but the PL luminance intensity decreases. As the dopant concentrate increases, the surface barrier becomes higher and the region space charge becomes narrower [32]. Figure S5 displays life time decays of ZnO bare and Sm–ZnO–Ag Nps. This life time decay shows the participation of equilibrated excited states accountable for emission. The photogenerated charge carriers could be comfortable to the deep-trap levels related to the oxygen vacancies of the nanostructure and as a result reunite radiatively with a much longer lifetime of Sm–ZnO–Ag Nps (Table 1). Therefore, Sm–ZnO–Ag is expected to exhibit higher photocatalytic activity compared to Ag–ZnO and Sm–ZnO Nps.

### Photodegradability of MB

The photodegradability of MB with the various photocatalysts using LED irradiation is shown in Fig. 7. 8% Sm–ZnO–Ag shows excellent and maximum degradation of dyes using LED within 80 min.

In the absence of LED, only a 10.1% decrease in dye concentration is observed in same circumstance and in the same catalyst. Very low degradation of 0.2% obtained in the absence of catalyst with LED. The adsorption principle played a vital role in this degradation. From the above discussion, for complete and effective degradation, we confirm both catalyst and LED light as mandatory. When the photocatalysts, such as Ag–ZnO, 8% Sm–ZnO–Ag, 4% Sm–ZnO–Ag, 2% Sm–ZnO–Ag, and bare ZnO Nps were used under the same conditions, 75.4, 96.9, 92.3, 86.436, and 69.62% of degradations occurred, respectively (Fig. 8). From this, we can conclude that 8% Sm–ZnO–Ag Nps is more efficient competent when compared to related catalysts in MB degradation.

### Influence of operational parameters

#### Effect of solution pH

The dye was adsorbed on the surface of the catalyst for the photodegradation and it is influenced by pH of the solution,

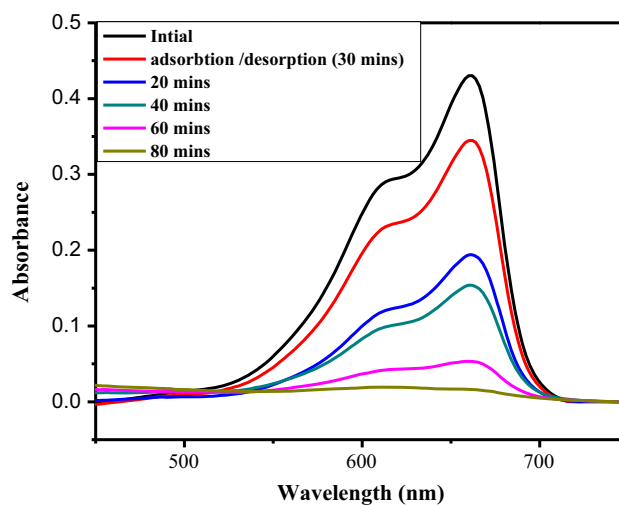


**Fig. 7** UV–Vis spectra on irradiation of MB with LED light in the presence of 8% Sm–ZnO–Ag. [MB] =  $10^{-5}$  M, pH = 11, and catalyst suspension =  $0.5 \text{ g L}^{-1}$  at different time intervals

hence pH plays an important role in photodegradation (Fig. 9 and S2). The MB degradation increased (10.1–96.21%) when the pH was raised linearly from lower to higher (3–11). The excellent degradation was observed at pH = 11 due to the radical formation, at the acidic pH, the degradation is very less because of dissolution of catalyst. The percentages of degradation of MB at different pH 3, 5, 7, 9 and 11 were found to be 10.1, 16.4, 22.71, 43.21 and 96.21%, respectively, after the adsorption equilibrium (30 min) in all responses. At pH 11, the adsorption and degradation were high. At pH 11, medium Sm–ZnO–Ag catalyst was negatively charged by means of adsorbed  $\text{HO}^-$  ions. The enormous amount of  $\text{HO}^-$  ions in the particle surface and in reaction medium helped in for the radical formation  $\text{HO}^-$  [27, 28].

#### Effect of catalyst dosage

It is strongly understood that the degradation of dye depends on the catalyst loading in the system. Experiments conducted with various amounts of 8% Sm–ZnO–Ag Nps explained that the photodegradation capacity decreased

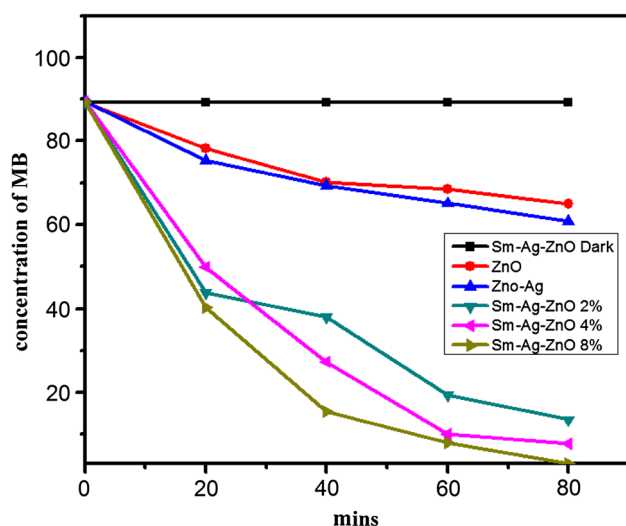


**Fig. 8** Photodegradability of MB dye. Dye concentration =  $10^{-5}$  mol  $L^{-1}$ , catalyst suspension =  $0.5 \text{ g } L^{-1}$ , and pH = 11 with ZnO bare and Sm–ZnO–Ag Nps

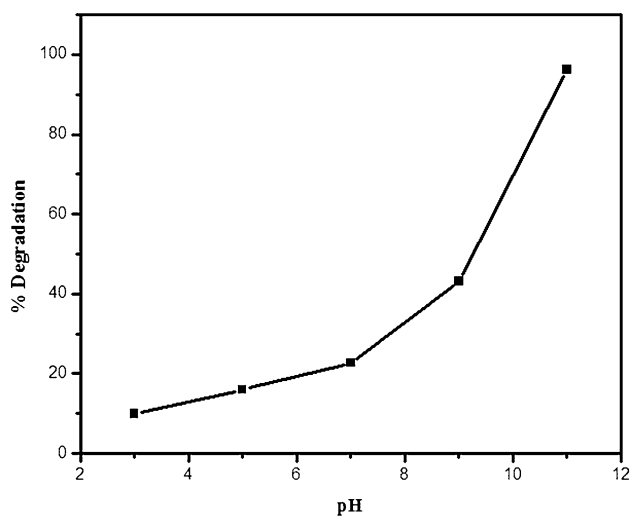


**Fig. 9** Effect of solute ion pH. [MB] =  $10^{-5}$  M  $L^{-1}$ , 8 wt % Sm–ZnO–Ag Nps, catalyst suspension =  $500 \text{ mg } L^{-1}$ , and irradiation time = 80 min

with an increase in the amount  $0.5\text{--}2 \text{ g } L^{-1}$  (Figs. 10, S3) and then slightly increases at  $2.5 \text{ g } L^{-1}$ . The best catalyst loading was found to be  $0.5 \text{ g } L^{-1}$ . The increased degradation of dye for  $0.5 \text{ g } L^{-1}$  was due to the amount of dye adsorbed on the surface of the catalyst. The decrease in the degradation efficiency of MB for higher yield may be due to dosage effect by the catalyst. Similar results were obtained for photodegradation of dyes by ZnO [29–31].

#### Effect of initial dye concentration

Photodegradation major influence depends on the initial concentration of MB dyes. A photodegradation realized by

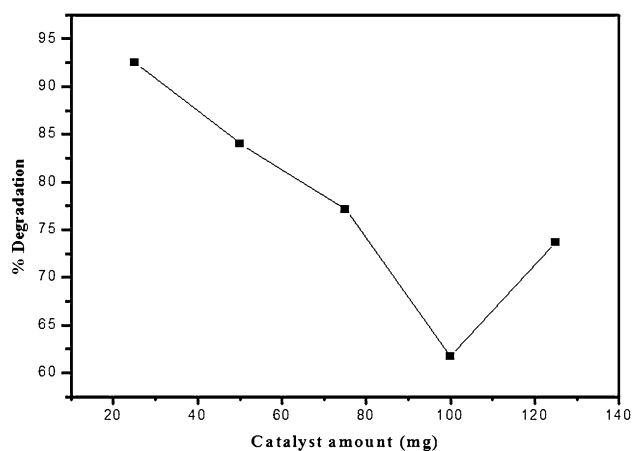


**Fig. 10** Effect of catalyst loading. [MB] =  $10^{-5}$  mol  $L^{-1}$ , catalyst used = 8 wt% Sm–ZnO–Ag Nps, pH = 11, and irradiation time = 80 min

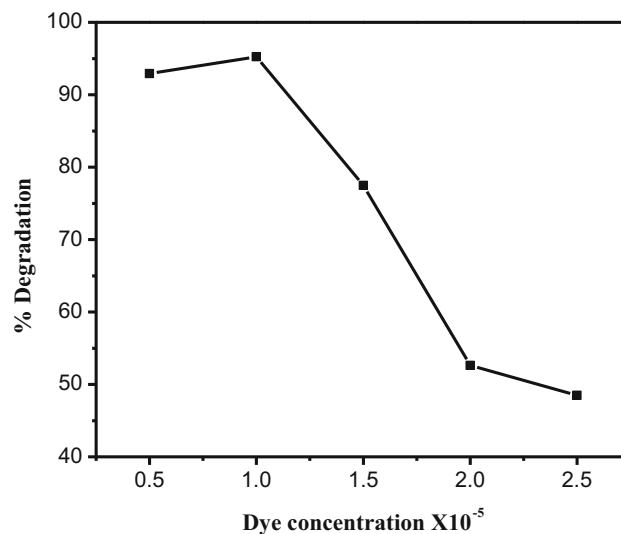


**Fig. 11** The effect of initial concentration of MB on irradiation with LED light in the presence 8% Sm–ZnO–Ag Nps. pH = 11, and catalyst suspension =  $0.50 \text{ g } L^{-1}$  at different initial concentrations

various initial concentrations of MB with 8% Sm–ZnO–Ag Nps (Figs. 11, S1) was investigated. Influence of MB concentration from  $0.5$  to  $2.59 \times 10^{-5}$  mol/L ( $50 \text{ mg}$  of catalyst), the photodegradation percentage is 95.23–48.49% it was absorbed at 80 min of irradiation

MB dye  $\rightarrow$  Absorbed by surface of catalyst  
 $\rightarrow$  Intermediate pds  $\rightarrow$  Non - toxic pds.

The hydroxyl radical  $HO^{\cdot}$  was formed over the catalyst surface, and that  $HO^{\cdot}$  radical was responsible for the rate of dye degradation [31–36]. Moreover, an influence of initial concentration of MB and the pathway length of the photons entering the solution decreases; low yield of  $HO^{\cdot}$  radical also leads to reduced yield of degradation efficiency.

**Table 2** Antibacterial and antifungal assessment of ZnO bare and Sm–ZnO–Ag Nps

| S. no. | Name of the microorganisms    | ZnO bare | Ag–ZnO | 2% Sm–ZnO–Ag | 4% Sm–ZnO–Ag | 8% Sm–ZnO–Ag |
|--------|-------------------------------|----------|--------|--------------|--------------|--------------|
| 1      | <i>Pseudomonas aeruginosa</i> | ++       | ++     | ++           | ++           | +++          |
| 2      | <i>Fusarium oxysporum</i>     | –        | –      | –            | –            | –            |
| 3      | <i>Aspergillus niger</i>      | –        | +      | –            | +++          | ++           |
| 4      | <i>E. coli</i>                | ++       | ++     | ++           | ++           | +++          |
| 5      | <i>Enterococcus faecium</i>   | +        | ++     | +++          | +++          | +++          |

Excellent: +++ (4 mm), good: ++ (3 mm), fair: + (1.5 mm), poor: (0)

### Antimicrobial studies

The results of the quantitative antibacterial and antifungal assessment by agar diffusion are shown in Table 2. It is observed that the size of the inhibition zone is higher in *Pseudomonas* species. It was found that *Enterococcus faecium* was significantly affected when comparing with other species. *Fusarium oxysporum* did not show any sensitivity comparative data with other species mentioned (Table 2). *Enterococcus* and *Pseudomonas sp* from bacteria and *Aspergillus sp* from fungi showed higher inhibition rate at a range of 4 and 8% Sm–ZnO–Ag Nps. Based on its zone formation, which shows that it has more doping (Ag/Sm), enhances the antibacterial and antifungal activity. However, the organism *E. coli* showed little difference in its zone of inhibition at 4 and 8% Sm–ZnO–Ag Nps. *E. coli* showed a negligible response towards the concentration, where a faint zone of inhibition and radical generation was observed. The small size allows the nanoparticles to cross the cell wall of the bacteria disrupting the cell membrane and leading to cell death. Also, the degree of dispersion of nanoparticles in water plays an important role in the antibacterial mechanism, and it increases with decrease in particle size. Therefore, the improved antibacterial properties of the samples with smaller silver content may be recognized to the enlarged surface to volume ratio which provides them better contact with the bacterial cell [29]. Moreover, during the course of the experiment, a very important observation was noted that antibacterial and fungal action was greatly enhanced when they were charged with more than 2% concentration and generation of free radicals although growth on agar plates is a maximum means of observing the antibacterial and fungal properties. Based on its zone diameter, *Enterococcus* and *Pseudomonas sp* show a excellent catalyst activity [29, 37–39].

### Sunlight photodegradation of MB

The irradiation of the MB dye using solar light (everyday 11 A.M.–3 P.M.) was done, and a complete degradation (Fig. 12) was obtained within 10 min (video attached in

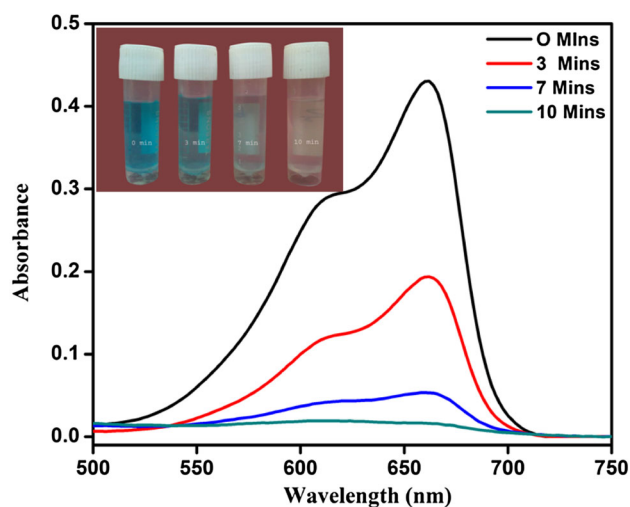


**Fig. 12** UV–Vis spectra on irradiation of MB with solar light in the presence of 8% Sm–ZnO–Ag Nps. [MB] =  $10^{-5}$  M, pH = 11, and catalyst suspension =  $0.5 \text{ g L}^{-1}$  at different time intervals

supporting documents) with 8% Sm–ZnO–Ag NPs under solar illumination. The experiments of photodegradability of MB were carried out in same conditions for both sunlight and LED. Sunlight (10 min) gave excellent results in the photocatalytic degradation when compared to LED (80 min). Similarly, solar light photodegradations of Azo dyes were observed in Ce (40 min) [25] Zr (40 min) [26] doped Ag–ZnO. We could observe that of MB 10% MB dye is absorption/desorption occurred in the experiment performed with 8% Sm–ZnO–Ag (without solar light). Just 2% degradation in dye concentration was absorbed when the experiment was performed on solar light (without catalyst). More efficient photodegradation of the MB dye depended on light and catalysts. The photocatalysts bare ZnO, Ag–ZnO, Sm–ZnO–Ag Nps were used under the same conditions, 60, 65.9, 85.3, 91.4, 100% degradations happen (Fig. 13), respectively. The 8% Sm–ZnO–Ag catalyst is excellent and efficient when compared to related catalyst for photodegradation of MB (Fig. 14). From this, we can clearly say that the solar degradation is much better than LED degradation. Within 10 min (video is attached in the supporting document), the

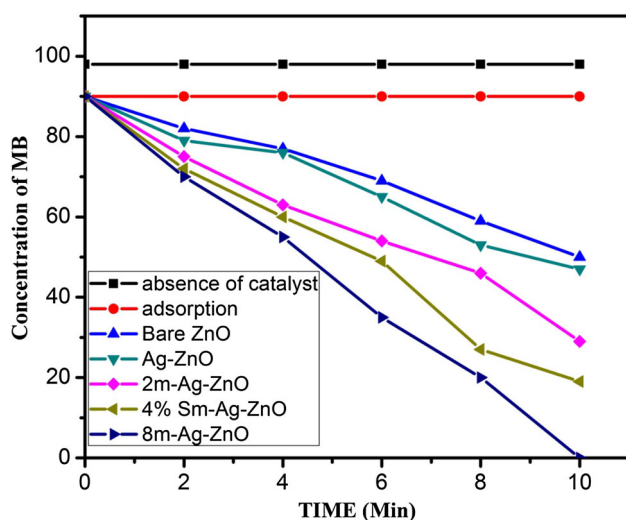


**Fig. 13** Photodegradability of MB dye. Dye concentration =  $10^{-5}$  mol L $^{-1}$ , catalyst suspension =  $0.5$  g L $^{-1}$ , and pH = 11 with different photocatalysts in the presence of solar light

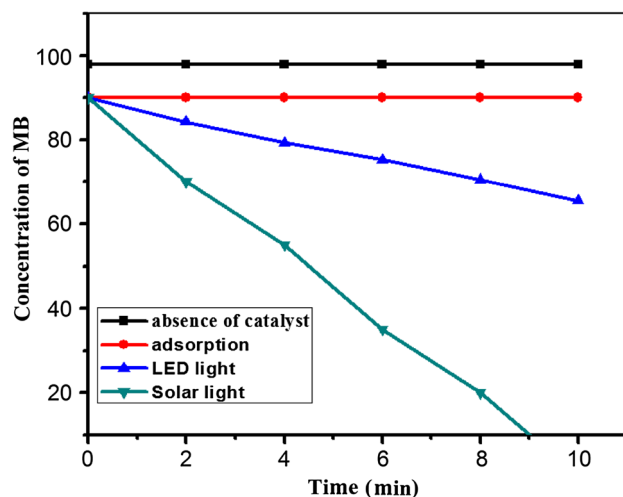


**Fig. 14** Comparison of photodegradability of MB between solar and LED lights. Dye concentration =  $10^{-5}$  mol L $^{-1}$ , catalyst suspension =  $0.5$  g L $^{-1}$ , and pH = 11 with 8% Sm-ZnO-Ag

degradation was completed for solar light, whereas the degradation took place 80 min for completion with LED under the same conditions.

### Catalyst reusability

In our studies, we have seen that heterogeneous photocatalyst can be reused and photocatalyst also found to be reusable. An experiment was performed in continuous four cycles for the photodegradation of MB dyes (Fig. 15) under LED/solar light. For the first three runs, we got complete degradation within 80 min, and for the last run, we got 95.6% degradation with the same time. Similar

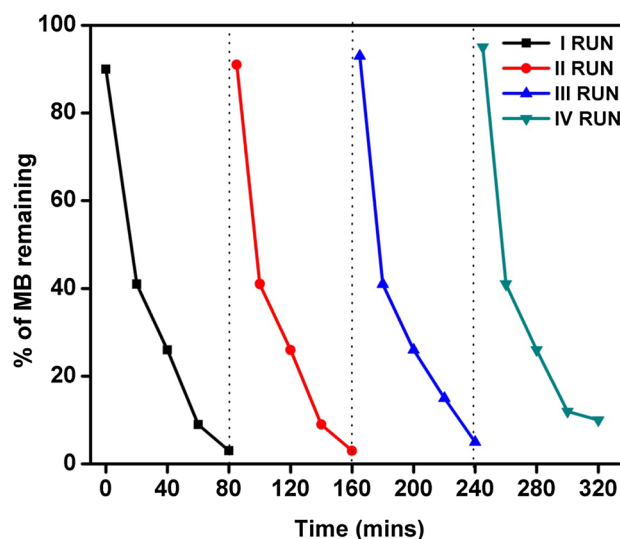


**Fig. 15** Catalyst reusability: [MB] dye concentration =  $10^{-5}$  mol L $^{-1}$ , catalyst 8% Sm-ZnO-Ag Nps =  $0.5$  g L $^{-1}$ , pH = 11, Light sources: LED and solar

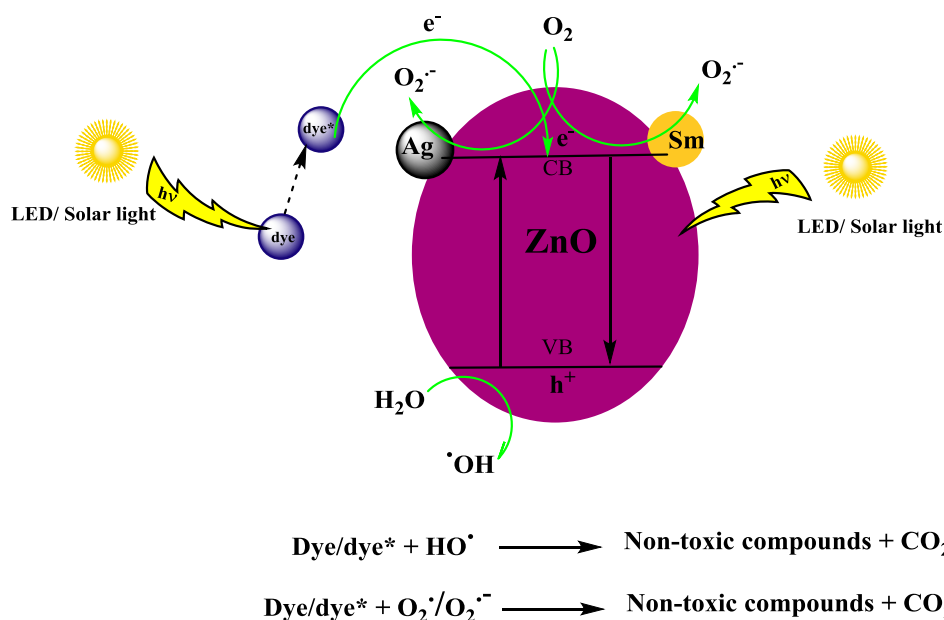
results were found to be in solar degradation [27]. Heterogenous catalyst had no such loss of activity till the 4th run and the photocatalyst was found to be stable and reusable.

### Mechanism of photodegradation

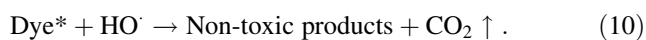
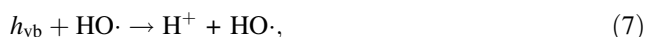
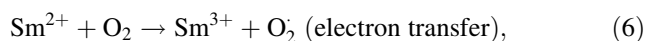
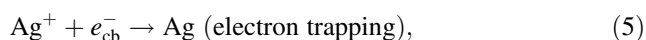
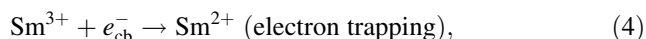
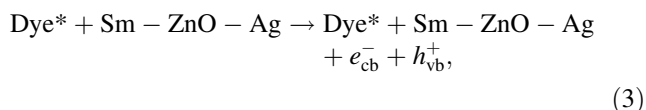
A postulated mechanism was proposed for the photodegradation of MB by the synthesized Sm-ZnO-Ag catalysis as shown in Scheme 2. Under the irradiation of MB dye in LED/solar light is to excited the dye molecules and excited catalyst having the electrons were excited to the conduction (CB) band from the valence (VB) band forming a hole in the VB (Eqs. 2–5). The electron holes are combined again to diminish the photocatalytic property of semiconductors. This is the reason why we are using dopants (Sm/Ag) with ZnO catalyst. These dopants help in increasing the photocatalytic properties. The Sm and Ag trap the electron in the conduction band and reduce the recombination of electron-hole pair. Sm $^{3+}$  doping helps ZnO to act as a strong Lewis acid because of the presence of half-filled 4f orbital which can efficiently capture the electron. Thus, the electron-hole recombination was suppressed. Sm $^{3+}$  is reduced to Sm $^{2+}$ . This reduced Sm $^{2+}$  is unstable, and therefore, the electrons are readily oxidized and given to the O $_2$  molecules promoting O $_2^-$  formation. Sm and silver dopants act as an active charge carrier trap and facilitate the excited electron transfer on LED/solar light (Eqs. 4–8).

During this time, the photogenerated  $h_{vb}^+$  could transfer the charge to the adsorbed H $_2$ O molecule or with surface recoil HO $\cdot$  species, by capturing the catalyst surface to

**Scheme 2** Enhanced photocatalytic activity mechanism of Sm–ZnO–Ag Nps in the presence of LED/solar lights



generate active  $\text{HO}^\cdot$  species. It conformed to dye-sensitized mechanism approached dye molecules, it can be converted to by-products. (Eqs. 9, 10). The steps are shown below:



## Conclusions

The Sm–ZnO–Ag catalysis was productively synthesized via precipitation–decomposition technique. The elements composition and physical properties (Sm, Ag, ZnO) were studied by FE-SEM, EDS, XRD, DRS, and optical spectra. The absorption peak of ZnO Nps was shifted into the visible region by (Sm and Ag) the dopants; Sm–ZnO–Ag Nps have inferior reflectance in the visible region compared to ZnO Nps. This lowered reflectance has increased absorption in the visible area. PL spectra proved the inhibition of recombination of electron–hole pair by

the dopants Ag and Sm on ZnO Nps. The role of the dopants Ag and  $\text{Sm}^{3+}$  was to trap the photoexcited electron by reducing the electron–hole recombination, which increases the photocatalytic properties. 8% Sm–ZnO–Ag Nps shows excellent photocatalytic activity than 4% Sm–ZnO–Ag, 2% Sm–ZnO–Ag, Ag–ZnO, and Bare ZnO Nps for the photodegradation of methylene blue dye under LED light. The optimum pH, catalytic dosage and concentration of dye were found to be 11, 500, and  $0.5 \times 10^{-5} \text{ molL}^{-1}$ , respectively. Light emitting diodes were used to complete the degradation of methylene blue dye. Sunlight showed excellent activity compared to that LED in the photodegradation of MB dye. Microbes zone size increased by microorganism growth due to radical ( $\text{O}_2^\cdot$  and  $\text{HO}^\cdot$ ) generation effect of Sm–ZnO–Ag Nps. The results were recommended that Sm–ZnO–Ag catalyst can be used efficiently against microbial growth. A clear mechanism was suggested, where Ag and Sm trap the electron. This shows an excellent performance of the photocatalyst. Moreover, Sm–ZnO–Ag was said to be stable.

**Acknowledgements** The author Dr. SJS is thankful to the management and principal of St. Josephs College Tiruchirappalli-620002 for their support and encouragement. The authors YJJ and Dr. MM are thankful to the management and principal of BWDA Arts and Science College Tindivanam-604304 for providing lab facilities.

**Open Access** This article is distributed under the terms of the Creative Commons Attribution 4.0 International License (<http://creativecommons.org/licenses/by/4.0/>), which permits unrestricted use, distribution, and reproduction in any medium, provided you give appropriate credit to the original author(s) and the source, provide a link to the Creative Commons license, and indicate if changes were made.



## References

1. Gaya, U.I., Abdullah, A.H.: Heterogeneous photocatalytic degradation of organic contaminants over titanium dioxide. *J. Photochem. Photobiol. C* **9**, 1–12 (2008)
2. Lazar, M.A., Varghese, S., Nair, S.S.: Photocatalytic water treatment by titanium dioxide. *Catalysts* **2**, 572–601 (2012)
3. Pan, H.M., Feng, J.H., He, G.X., Cerniglia, C.E., Chen, H.Z.: Evaluation of impact of exposure of Sudan azo dyes and their metabolites on human intestinal bacteria. *Anaerobe* **18**, 445–453 (2012)
4. Vautier, M., Guillard, C., Herrmann, J.M.: Photocatalytic degradation of dyes in water: case study of indigo and of indigo carmine. *J. Catal.* **201**, 46–59 (2001)
5. Chang, M.W., Chung, C.C., Chern, J.M., Chen, T.S.: Dye decomposition kinetics by UV/H<sub>2</sub>O<sub>2</sub>: initial rate analysis by effective kinetic modeling methodology. *Chem. Eng. Sci.* **65**, 135–140 (2010)
6. Chakrabarti, S., Dutta, B.K.: Photocatalytic degradation of model textile dyes in wastewater using ZnO as semiconductor catalyst. *J. Hazard. Mater.* **112**, 269–278 (2004)
7. Rao, A.N., Sivasankar, B., Sadasivam, V.: Kinetic studies on the photocatalytic degradation of Direct Yellow 12 in the presence of ZnO catalyst. *J. Mol. Catal. A* **306**, 77–81 (2009)
8. Priyragini, S., Veena, S., Swetha, D., Karthik, L., Kumar, G., Bhaskara Rao, K.V.: Evaluating the effectiveness of marine actinobacterial extract and its mediated titanium dioxide nanoparticles in the degradation of azo dyes. *J. Environ. Sci.* **26**, 775–782 (2014)
9. Aleboyeh, A., Kasiri, M.B., Aleboyeh, H.: Influence of dyeing auxiliaries on AB74 dye degradation by UV/H<sub>2</sub>O<sub>2</sub> process. *J. Environ. Manage.* **113**, 426–431 (2012)
10. Huang, H.B., Leung, D.Y.C., Kwong, P.C.W., Xiong, J., Zhang, L.: Enhanced photocatalytic degradation of methylene blue under vacuum ultraviolet irradiation. *Catal. Today* **201**, 189–194 (2013)
11. Surolia, P.K., Lazar, M.A., Tayade, R.J., Jasra, R.V.: Photocatalytic degradation of 3,3'-dimethylbiphenyl-4,4'-diamine (*o*-tolidine) over nanocrystalline TiO<sub>2</sub> synthesized by sol–gel, solution combustion, and hydrothermal methods. *Ind. Eng. Chem. Res.* **47**, 5847–5865 (2008)
12. Rogozea, E.A., Meghea, A., Olteanu, N.L., Bors, A., Mihaly, M.: Fullerene-modified silica materials designed for highly efficient dyes photodegradation. *Mater. Lett.* **151**, 119–121 (2015)
13. Chen, H.W., Ku, Y., Wu, C.Y.: Effect of LED optical characteristics on temporal behavior of *o*-cresol decomposition by UV/TiO<sub>2</sub> process. *J. Chem. Technol. Biotechnol.* **82**, 626–635 (2007)
14. Daniel, D., Gutz, I.G.R.: Microfluidic cell with a TiO<sub>2</sub>-modified gold electrode irradiated by an UV-LED for in situ photocatalytic decomposition of organic matter and its potentiality for voltammetric analysis of metal ions. *Electrochem. Commun.* **9**, 522–528 (2007)
15. Ge, M., Chen, Y., Liu, M., Li, M.: Synthesis of magnetically separable Ag<sub>3</sub>PO<sub>4</sub>/ZnFe<sub>2</sub>O<sub>4</sub> composite photocatalysts for dye degradation under visible LED light irradiation. *J. Environ. Chem. Eng.* **3**, 2809–2815 (2015)
16. Hu, J.S., Ren, L.L., Guo, Y.G., Liang, H.P., Cao, A.M., Wan, L.J., Bai, C.L.: Mass production and high photocatalytic activity of ZnS nanoporous nanoparticles. *Angew. Chem. Int. Ed.* **44**, 1269–1273 (2005)
17. Gnanasekaran, L., Hemamalini, R., Ravichandran, K.: Synthesis and characterization of TiO<sub>2</sub> quantum dots for photocatalytic application. *J. Saudi Chem. Soc.* **19**, 589–594 (2015)
18. Fujishima, A., Honda, K.: Electrochemical photolysis of water at a semiconductor electrode. *Nature* **238**, 37–38 (1972)
19. Linsebigler, A.L., Lu, G.Q., Yates, T.J.: Photocatalysis on TiO<sub>2</sub> surfaces: principles, mechanisms, and selected results. *Chem. Rev.* **95**, 735–738 (1995)
20. Nakata, K., Fujishima, A.: TiO<sub>2</sub> photocatalysis design and applications. *J. Photochem. Photobiol. C* **13**, 169–189 (2012)
21. Zhao, N., Yao, M., Lia, F., Lou, F.: Microstructures and photocatalytic properties of Ag<sup>+</sup> and La<sup>3+</sup> surface codoped TiO<sub>2</sub> films prepared by sol–gel method. *J. Solid State Chem.* **184**, 2770–2775 (2011)
22. Sin, J.C., Lam, S.M., Lee, K.T., Mohamed, A.R.: Photocatalytic performance of novel samarium-doped spherical-like ZnO hierarchical nanostructures under visible light irradiation for 2,4-dichlorophenol degradation. *J. Colloid. Interface. Sci.* **401**, 40–49 (2013)
23. Saravanan, R., Shankar, H., Prakash, T., Narayanan, V., Stephen, A.: ZnO/CdO composite nanorods for photocatalytic degradation of methylene blue under visible light. *Mater. Chem. Phys.* **125**, 277–280 (2011)
24. Gnanasekaran, L., Hemamalini, R., Saravanan, R., Ravichandran, K., Gracia, F., Gupta, V.K.: Intermediate state created by dopant ions (Mn, Co and Zr) into TiO<sub>2</sub> nanoparticles for degradation of dyes under visible light. *J. Mol. Liq.* **223**, 652–659 (2016)
25. Subash, B., Krishnakumar, B., Velmurugan, R., Swaminathan, M., Shanthi, M.: Synthesis of Ce co-doped Ag–ZnO photocatalyst with excellent performance for NBB dye degradation under natural sunlight illumination. *Catal. Sci. Technol.* **2**, 2319–2326 (2012)
26. Kaneva, N.V., Dimitrov, D.T., Dushkin, C.D.: Highly active Zr co-doped Ag–ZnO photocatalyst for the mineralization of acid black 1 under UV-A light illumination. *Appl. Surf. Sci.* **257**, 8113–8120 (2011)
27. Jo, W.K., Tayade, R.J.: Recent developments in photocatalytic dye degradation upon irradiation with energy-efficient light emitting diodes. *Chin. J. Catal.* **35**, 1781–1792 (2014)
28. Jo, W.K., Tayade, R.J.: New generation energy-efficient light source for photocatalysis: LEDs for environmental applications. *Ind. Eng. Chem. Res.* **53**, 2073–2084 (2014)
29. Gilbert, P., Brown, M.R., Costerton, J.W.: Inocula for antimicrobial sensitivity testing: a critical review. *J. Antimicrob. Chemother.* **20**, 147–154 (1987)
30. Mosleh, S., Rahimi, M.R., Ghaedi, M., Dashtian, K., Hajati, S., Wang, S.: Ag<sub>3</sub>PO<sub>4</sub>/AgBr/Ag-HKUST-1-MOF composites as novel blue LED light active photocatalyst for enhanced degradation of ternary mixture of dyes in a rotating packed bed reactor. *Chem. Eng. Process. Process Intensif.* **114**, 24–38 (2017)
31. Saravanan, R., Karthikeyan, N., Gupta, V.K., Thirumal, E., Thangadurai, P., Narayanan, V., Stephen, A.: ZnO/Ag nanocomposite: an efficient catalyst for degradation studies of textile effluents under visible light. *Mater. Sci. Eng. C* **33**, 2235–2244 (2013)
32. Anandan, S., Vinu, A., Mori, T., Gokulakrishnan, N., Srinivasu, P., Murugesan, V., Ariga, K.: Photocatalytic degradation of 2,4,6-trichlorophenol using lanthanum doped ZnO in aqueous suspension. *Catal. Commun.* **8**, 1377–1382 (2007)
33. Velmurugan, R., Selvam, K., Krishnakumar, B., Swaminathan, M.: An efficient reusable and antiphotocorrosive nano ZnO for the mineralization of Reactive Orange 4 under UV-A light. *Sep. Purif. Technol.* **80**, 119–124 (2011)
34. Rogozea, E.A., Petcu, A.R., Olteanu, N.L., Lazar, C.A., Cadar, D., Mihaly, M.: Tandem adsorption-photodegradation activity induced by light on NiO-ZnO p–n couple modified silica nanomaterials. *Mater. Sci. Semicond. Process.* **57**, 1–11 (2017)

35. Krishnakumar, B., Selvam, K., Velmurugan, R., Swaminathan, M.: Influence of operational parameters on photodegradation of Acid Black 1 with ZnO. *Desalin. Water. Treat.* **24**, 132–139 (2010)
36. Olteanu, N.L., Rogozea, E.A., Popescu, S.A., Petcu, A.R., Lazăr, C.A., Meghea, A., Mihaly, M.: “One-pot” synthesis of Au–ZnO–SiO<sub>2</sub> nanostructures for sunlight photodegradation. *J. Mol. Catal. A: Chem.* **414**, 148–159 (2016)
37. Yadavalli, T., Shukla, D.: Role of metal and metal oxide nanoparticles as diagnostic and therapeutic tools for highly prevalent viral infections. *Nanomedicine. NBM* **13**, 219–230 (2017)
38. Giménez-Marqués, M., Hidalgo, T., Serre, C., Horcajada, P.: Nanostructured metal–organic frameworks and their bio-related applications. *Coord. Chem. Rev.* **307**, 342–360 (2016)
39. Balusamy, B., Kandhasamy, Y.G., Senthamizhan, A., Chandrasekaran, G., Subramanian, M.S., Kumaravel, T.S.: Characterization and bacterial toxicity of lanthanum oxide bulk and nanoparticles. *J. Rare Earths* **30**, 1298–1302 (2012)

